International Journal of ISSI, Vol.5 (2008), No. 2, pp. 29-35

research note

Evaluation of Nitrogen Diffusion in Plasma Nitrided Iron by Various Characterization Techniques

S. R. Hosseini[1*] and F. Ashrafizadeh[2]

1- Department of Materials Engineering, Maleke-ashtar University of Technology, 83145-115, Iran

2- Department of Materials Engineering, Isfahan University of Technology, Isfahan 84156-83111, Iran

Abstract

Diffusion of nitrogen in plasma nitrided iron and structural evolution during the nitriding process were evaluated by several characterization techniques including optical microscopy (OM), microhardness depth profiling (HDP), scanning electron microscopy (SEM), x-ray diffraction (XRD), glow discharge optical emission spectroscopy (GDOES), and secondary ion mass spectroscopy (SIMS). Plasma nitriding was carried out on high purity iron substrate at a temperature of 550°C in an atmosphere of 75%H_2-25%N_2. Case depth, thickness of the compound layer, micro-hardness profile, nitrogen depth profile, and characteristics of intermediate nitrides including epsilon, gamma prime, and $Fe_{16}N_2$ were studied. The results of characterization of plasma nitrided iron indicated a good agreement with experimental findings; thus, the techniques confirmed one another. For accurate measurement of nitrogen within the diffusion zone, where concentration was below 0.1wt%, secondary ion mass spectroscopy technique was used. The extent of nitrogen diffusion detected by secondary ion mass spectroscopy in this work was greater than 1800 μm; a value which is not reported in the literature.

Keywords: Nitrogen diffusion, Plasma nitriding, Pure iron, GDOES, SIMS.

1- Introduction

Nitriding is a thermo-chemical, case hardening process whereby nitrogen is introduced into the surface of a solid metal by holding the metal at a moderate temperature in contact with a nitrogenous medium [1)]. Understanding the process and controlling the nitrided structures are of great industrial interest because of the enhanced resistance of engineering components against wear, corrosion, and fatigue. Among the several processes available for improving surface properties, the plasma nitriding technique allows for better control of diverse parameters, thus permitting the formation of optimized layers [2)]. Although this process has been applied for many years to surface modification of iron, titanium, aluminum, and their alloys, revealing knowledge and data on the true relationships among plasma parameters, gas mixtures, and final properties yet remain to be obtained [3)].

Over the last two decades, extensive research has been carried out to better understand the Fe–N system and its relation to mechanical and tribological properties of the nitrided components [4-10)]. According to the Fe–N phase diagram [8)], maximum nitrogen content that can be dissolved in α-Fe is approximately 0.1 wt%. However, during the nitriding process, nitrogen concentration increases towards the surface and precipitates are formed when the solubility limit of nitrogen is exceeded. Nitrogen saturation in the ferrite matrix during cooling leads to the formation of iron nitrides. The case structure of the nitrided iron may include a compound layer, a diffusion zone, and a transition section between them. This structure depends on several parameters such as concentration of alloying elements, nitriding time and temperature, and the composition of gas mixture [11)].

In gas nitriding, the chemical potential is given by the relationship between ammonia and hydrogen partial pressures, and reflects the capability of gas mixtures and temperatures for introducing nitrogen into the sample. The nitriding potential is linearly proportional to the thermodynamically well-defined nitrogen activity in the solid state if a local equilibrium is achieved between the gaseous atmosphere and the nitrogen in the solid state [12)]. If a high nitriding potential is used during the process, many nitrogen atoms will diffuse into the sample surface, giving way to thick compound layers of ε-$Fe_{2-3}N$ and γ′-Fe_4N iron nitrides and a deep diffusion zone in iron-based alloys. For gas nitriding, several studies have been carried out on the process details [12,13)]. On the other hand, complex reactions in the plasma and their unknown superposition determine

* *Corresponding author:*
Tel: +98-311-3912750 Fax: +98-311-3912752
E-mail: hosseinisr@ma.iut.ac.ir
Address: Dept. of Materials Engineering, Maleke-ashtar University of Technology, 83145-115, Iran
1.Assistant Professor
2. Professor

the nitrogen activity of the plasma. Direct observation of plasma reactions and correlation with materials' properties is still difficult. When nitrogen is transferred from the plasma to the surface of the substrate, processes similar to those in gas nitriding are expected to occur [3].

Recently, the authors conducted theoretical investigations and mathematical calculations on the nitriding process [14-16]. To verify experimentally the structures formed during the plasma nitriding of pure iron, various techniques of optical and scanning electron microscopy, X-ray diffraction, and glow discharge optical emission spectroscopy were employed to characterize the morphology, phases, hardness profile, case depth, and elemental concentration depth profiles. Nevertheless, no published work is reported on accurate characterization of nitrogen diffusion in the alpha zone depths. For high precision mass concentration depth profiling of nitrogen from the surface through the depth of the substrate, secondary ion mass spectroscopy technique was used in conjunction with glow discharge optical spectroscopy. Nitrogen depth profile, detected by secondary ion mass spectroscopy technique is compared with other methods and the relations are discussed in terms of diffusion process.

2- Experimental procedures

2-1- Substrate preparation and nitriding procedure

Disc-shaped ARMCO iron samples 25 mm in diameter and 5mm thick were prepared from bars 30mm diameter. Table 1 shows the chemical composition and impurity levels of the substrate material. All specimens were ground by a flat magnetic wheel machine followed by mechanical grinding by 80 to 600-grit abrasive papers. The average surface roughness (R_a) of the specimens, measured by a SM7 PROFILETEST, was about 0.11 μm. The specimens were cleaned in acetone and dried before plasma nitriding.

Plasma nitriding was carried out in a semi-industrial unit. The apparatus comprised of a vacuum chamber (550 mm inner diameter and 600 mm height), a thermocouple (adjusted into the sample), a power supply (5kw capacity), water circulation system, and control accessories. The general sequence of the plasma nitriding experiments started with sputter cleaning and heating the specimens to 550 °C (823 K) ±5 °C in an atmosphere of 50 vol.% H_2 and 50 vol.% Ar. Cleaning took place by ion sputtering in 0.01 Torr pressure of H_2-Ar mixture for approximately 10 min, after which the heating cycle was started. Upon reaching the prescribed temperature, the atmosphere was switched to a mixture of 75 vol. % H_2 and 25 vol. % N_2 when the nitriding cycle began. The total gas pressure was about 5 Torr in all tests. The selected times were 1, 2, 5, and 10 hours. After the nitriding cycle was completed, the power supply was switched off and the samples were allowed to cool in the furnace under vacuum. Samples were collected from the chamber at room temperature.

2- 2- Analysis of the surface

Metallographic examinations were performed on cross sections of the samples prepared by a standard grinding and polishing procedure. After plasma nitriding, some samples were sectioned, nickel electroplated in the Watts plating bath, mounted in bakelite, ground, polished (0.3 μm Al_2O_3), and etched with 2% Nital solution. Microstructural observations were carried out using optical (OM) and scanning electron microscope (SEM), Philips XL 30. A thin layer of gold was sputtered on the surface of the samples to increase electron conduction in the scanning electron microscope chamber.

Microhardness depth profile (HDP) was performed on the cross section of plasma nitrided samples by using a ZWICK 3212 Vickers micro-hardness tester at an applied load of 50 g. f. Case depth and thickness measurement of the nitrided layers and diffusion zone were carried out by hardness profiling, optical and scanning electron microscopes.

X-ray diffraction (XRD) analyses were performed by a PHILIPS X'Pert diffractometer. Cu Kα radiation ($K\alpha_1$ of 1.54056 Å and $K\alpha_2$ of 1.54439 Å) was employed. The X-ray generator was operated at 40 kV and 30 mA. The patterns were obtained with a 2θ step size of 0.04°, in the range of 20–140°, with a time per step of one second.

For characterization of the elements diffused into the substrate, glow discharge optical emission spectroscopy (GDOES), LECO GDS-750 QDP apparatus, was used.

For accurate measurement of nitrogen concentration, secondary ion mass spectrometry (SIMS) was used as a new approach. In order to obtain a nitrogen depth profile by secondary ion mass spectrometry, mechanical sections through the sample surface were produced by cutting and sequential polishing and, then, point analyses were carried out on the surface. The data obtained were used to construct a concentration depth profile of nitrogen within the diffusion zone. Secondary ion mass spectrometry analyses were performed by using a CAMECA IMS 3f instrument. A section obtained from the sample using a diamond saw was polished. The secondary ion mass spectrometry line profile was obtained by taking data along a line in the sectioned surface normal to the original surface of the sample.

Table 1. Chemical composition and impurities of the ARMCO iron substrate material (wt %).

C	Si	Mn	Cr	Mo	Al	V	Ni	Cu	Ti	P	S	Fe
<0.0050	<0.0050	<0.050	<0.0100	<0.0080	<0.0080	0.0270	<0.030	0.0215	<0.0060	<0.0080	0.0090	99.81

3- Results and Discussion

Figure1 shows an optical micrograph and a general cross-sectional view of the structure of plasma nitrided iron. The compound layer, the diffusion zone, and the transition layer between them can be seen in this micrograph. Figure 2 illustrates scanning electron micrograph at a higher magnification of the structure of plasma nitrided iron. It can be seen that, although not shown in the optical micrograph, the compound layer is composed of two separate layers. Thickness of the outer layer is much smaller than that of the second one.

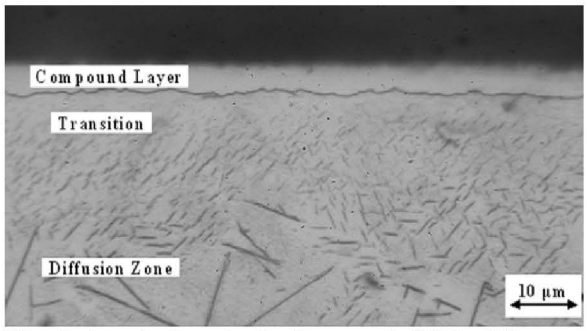

Fig. 1. A typical optical micrograph (OM) of the cross section of plasma nitrided iron.

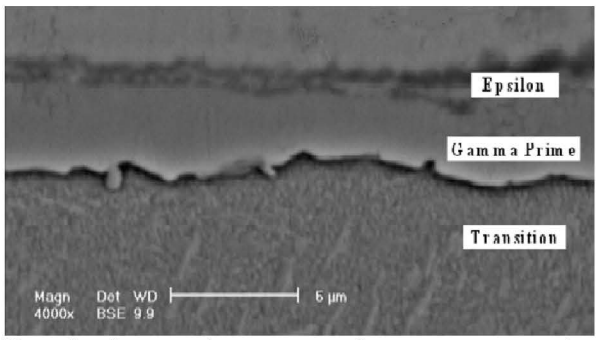

Fig. 2. A typical scanning electron micrograph (SEM) of the cross section of plasma nitrided iron.

Figure 3 shows XRD patterns of two plasma nitrided samples compared with that of untreated pure iron. For the untreated sample, there are five peaks diffracted from (110), (200), (211), (220), and (310) planes of pure iron. After one hour of plasma nitriding, several peaks appear from the epsilon and gamma prime nitrides. This means that one hour of plasma nitriding is enough for the formation of both epsilon and gamma prime nitrides. According to Sun and Bell [17], there is a threshold nitrogen potential at which the compound layer, epsilon and/or gamma prime nitrides, can be nucleated. For plasma nitriding of pure iron at a temperature of 560°C in an atmosphere containing at least 6vol%N_2, almost one hour is enough for the compound layer to nucleate. If nitrogen potential exceeds this limit, the incubation time for nucleation and growth of the compound layer decreases rapidly. In this research, plasma nitriding was performed at 550°C as also used by Sun and Bell [17]. The nitriding potential used in this investigation, however, was 25vol%N_2, which is far higher than that used in their calculations. At this nitriding potential, the compound layer can nucleate and grow in the initial stages of nitriding. Extrapolation of the curves extracted by Sun and Bell implies that if nitrogen percentage exceeds 15vol%, nitrides can nucleate and grow in 15 min.

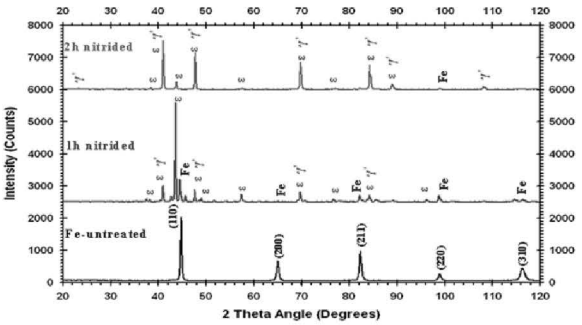

Fig. 3. X-ray diffraction (XRD) patterns of 1 and 2 h plasma nitrided samples compared to untreated iron.

It is clear from Figure 3 that since the epsilon nitride is the outer layer and the thickness of the gamma prime in the initial stages of nitriding is thin, the peaks of the epsilon nitride are stronger than those of the gamma prime nitride after one hour plasma nitriding. On the other hand, all five peaks from pure iron are diffracted after one hour plasma nitriding. This emphasizes the fact that both epsilon and gamma prime nitrides are quite thin in the primary stages of nitriding and thus x-ray radiation can penetrate through the compound layer. This result is in agreement with the metallographic examination and GDOES characterization.

After two hours of plasma nitriding, peaks of pure iron almost disappeared. This means that the compound layer was thick enough to act as a barrier to the penetration of x-ray radiation into the diffusion zone. Moreover, several peaks from the epsilon and gamma prime nitrides appeared. The strong peaks of the epsilon decreased after two hours of nitriding. In other words, the ratio of the epsilon peak height to that of the gamma prime decreased by increasing the nitriding time from one to two hours. Referring to the cross sectional microstructures, this phenomenon is caused by thickening of the gamma prime nitride that grows faster than that of the epsilon nitride. The growth rate of the compound layer (slope of the parabolic type equation) was found to be different for the epsilon and gamma prime nitrides at any nitriding temperature [16]. On the other word, at a given nitriding temperature, the growth rate of the gamma prime nitride was higher than that of the epsilon nitride. The main reason for this phenomenon is the diffusion coefficient of nitrogen. The magnitude of nitrogen diffusion coefficient in the alpha phase was about 100 times greater than that of the epsilon and 10 times that of the gamma prime nitride for any given temperature [15]. Moreover,

scanning electron microstructure (Figure 2) shows that thickness of the gamma prime nitride is 3-4 times higher than that of the epsilon nitride. This thick and continuous layer not only acts as a barrier to the penetration of x-ray beams toward the substrate, but also decreases the relative intensity of peaks of the outer thin layer, i.e. the epsilon nitride.

More XRD patterns were examined of the samples plasma nitrided at a temperature of 550°C for 5 and 10 hours. The results revealed that increasing the nitriding time up to 2h had a significant effect on XRD patterns, but that longer periods had no considerable influence. This indicated that nitriding time up to 2h resulted in the considerable growth of the compound layer. Moreover, a 2h nitriding cycle led to the establishment of the surface structure and increasing nitriding time had no considerable effect on microstructural variations. This phenomenon is in agreement with the parabolic growth rate.

A typical microhardness depth profile is demonstrated in Figure 4 for the sample plasma nitride for 2 hours at 550°C; hardness of the outer (compound) layer is higher than 1000 HV and decreases rapidly to below 300 HV at the transition zone. The hardness gradient decreases smoothly from the transition zone toward the substrate. The microhardness profile becomes almost constant at H_o, which is marked as the hardened case depth (Figure 4). Microhardness depth profile measurements were performed on the samples plasma nitrided at different time cycles and several hardened case depths were obtained. Moreover, microstructural changes near the plasma nitrided surface were studied by optical and scanning electron microscopes.

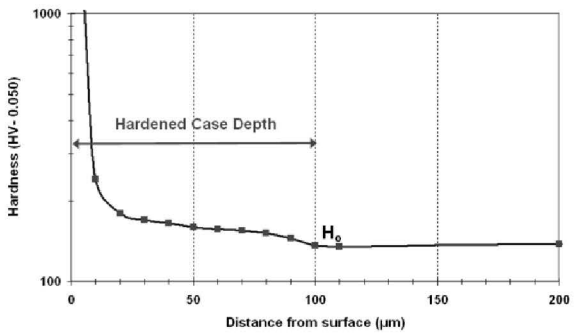

Fig. 4. A typical microhardness depth profile (HDP) of plasma nitrided iron.

Figure 5 demonstrates the case depth of the plasma nitrided samples measured by two methods at different nitriding times. The lower curve represents the hardened case depth measured by microhardness depth profile, while the upper one is based on the measurements made by scanning electron microscopy. At any given nitriding time, case depth measured by SEM is higher than that measured by the microhardness depth profile. This implies that not all the changes in the microstructure have significant effects on microhardness. Study of microstructures by optical and SEM revealed that precipitates with two different sizes and morphologies were dispersed from the transition zone towards the substrate. These two precipitate morphologies are evidenced on the optical micrograph in Figures 6 and 7. The coarse thicker precipitates are observed as random needles with a lower density while the fine thinner ones are distributed with a higher concentration in the matrix. Although coarse precipitates concentrated mostly near the compound layer and thinner ones formed far from the surface, these two kinds of precipitates are almost mixed together and their density decreases from the transition zone toward the substrate. These characteristics are consistent with the precipitates recently identified by Gontijo et al [2]. According to their identification which conforms to ours reported here, the two morphologies were nitrides with the stoichiometric formulae Fe_4N and $Fe_{16}N_2$ for coarse and fine precipitates, respectively.

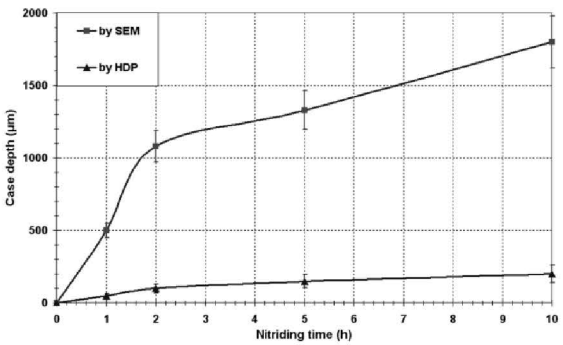

Fig. 5. Case depth of plasma nitrided iron at different nitriding periods, measured by scanning electron microscope (SEM) and microhardness depth profile (HDP).

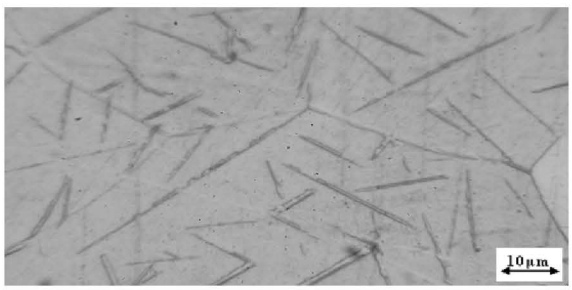

Fig. 6. Optical micrograph (OM) of the coarse and thicker precipitates.

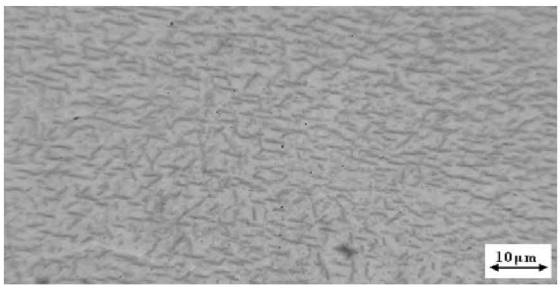

Fig. 7. Optical micrograph (OM) of the fine and thinner precipitates.

In order to account for the difference between case depths measured by microhardness depth profile and SEM as shown in Figure 5, one should note that the nitride precipitates near the surface are sufficiently high and concentrated together to increase the microhardness. Moving from the transition zone toward the substrate, the concentration of the nitride precipitates and, thereby, the gradient of the hardness profile decrease (Figure 4). Where the nitride precipitates concentration is not high enough to influence microhardness, H_o, the structural changes in the case depth cannot be measured by microhardness, they are rather evidenced by optical and scanning electron microscopy.

Concentration depth profiles of nitrogen and iron characterized by GDOES are shown in Figure 8. The profiles can be divided into three sections: at the outer section, the nitrogen concentration is very high, indicating that the compound layer was formed. At the inner section, nitrogen concentration decreases to nearly zero and that of iron increases to approximately 100 percent. This concentration corresponds to the diffusion zone. Between the compound layer and the diffusion zone, there is a transition section in which nitrogen concentration decreases with a smooth gradient. It seems that during the formation and growth of the compound layer, nitrogen can diffuse towards the substrate but cannot distribute in the alpha zone rapidly and thus, the transition zone is formed. The nitrogen concentration depth profile, Figure 8, is consistent with the optical and scanning electron micrographs in Figures 1 and 2.

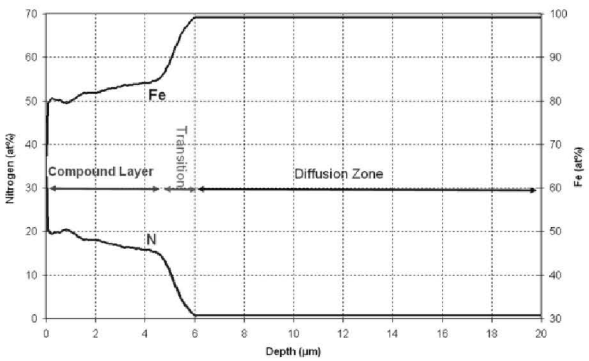

Fig. 8. Concentration depth profiles of nitrogen and iron characterized by glow discharge optical emission spectroscopy (GDOES).

To investigate the diffusion process, we needed to measure the depth profile for nitrogen within the diffusion zone where the nitrogen concentration was around zero. Samples were analyzed by GDOES and characterized several times. The results for the compound layer, where nitrogen concentration was relatively high, were acceptable but problems arose for the characterization of nitrogen at the diffusion zone. Maximum solubility of nitrogen and, thus, maximum nitrogen concentration at the alpha iron, i.e. in the diffusion zone, almost reached 0.1wt%. The predicted concentration of nitrogen decreases from 0.1wt% to 0.01wt% or even less at the depth of the substrate. Based on our calculations, the expected depth of the diffusion zone is much higher than that measured by GDOES [15].

Figure 9 shows a typical concentration depth profile of nitrogen characterized by secondary ion mass spectrometry. Nitrogen signals rose to above 1000 counts/second at the nitrided surface, decreasing rapidly to 200 counts/second at a depth of 60 µm, and then smoothly decreasing to nearly zero at a depth of about 1200 µm. Like the GDOES profile (Figure 8), at the outer section, nitrogen concentration was very high, indicating that the compound layer was formed. But, there are major differences between GDOES and SIMS profiles at the inner section. In the GDOES profile, Figure 8, nitrogen concentration decreased to nearly zero from a depth of 6 µm toward the substrate. This is while the SIMS profile (Figure 9) shows a very smooth gradient up to 1200 µm. This concentration corresponds to the diffusion zone that could not be detected by GDOES. According to SIMS results, during the formation and growth of the compound layer, nitrogen can diffuse towards the substrate and distribute deep in the alpha diffusion zone. The GDOES technique is normally capable of profiling elements to a depth of about 100 micrometers [18, 19]. If any element diffuses deeper than this, then the sample should be polished down after the initial profile and a further profile should be taken at the same position [20]. This procedure can be repeated several times and has been successfully used to profile through to about a millimeter, provided the concentration of the elements is high enough to be detected by GDOES. In cases where the concentration of nitrogen decreases to less than 0.1 wt%, i.e. below the sensitivity of GDOES, nitrogen concentration cannot be measured accurately.

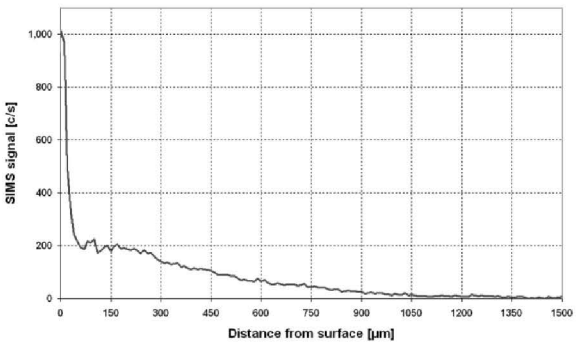

Fig. 9. Concentration depth profiles of nitrogen characterized by secondary ion mass spectroscopy (SIMS).

On the other hand, the depth profile detected by SIMS technique was much higher than the case depth measured by microhardness depth profile and SEM even at the 10h nitriding cycle (Figure 5). This indicated that nitrogen diffused to the end of the diffusion zone, but that the concentration of nitrogen

was not sufficient to form precipitates. Further examination by SIMS technique showed some weak and random nitrogen signals up to a depth of 2500 μm in the 10h nitrided samples. Investigations by optical and scanning electron microscopy of the plasma nitrided microstructure revealed that nitrogen diffused not only through the iron lattices but also through the grain boundaries. Grain boundary is known as a rapid diffusion path through which alloying elements can diffuse much faster than in the lattice [21]. Nitrogen diffused in the alpha iron depth by both lattice and grain boundary diffusion mechanisms.

Comparisons of the main changes in the plasma nitrided iron case under practical conditions evaluated by various characterization techniques are presented in Figure 10. The thickness of the compound layer is normally in the range of 2-10 μm, while the hardened case nearly reaches 150 μm. The thickness of the hardened case is much smaller than that of microstructural changes. Microstructural changes that can be evidenced by optical and electron microscopy are smaller than the continuous diffusion zone. Maximum depth of nitrogen diffusion, detected by SIMS technique, almost reaches 2500 μm while the depth of the continuous diffusion zone is about 1800 μm.

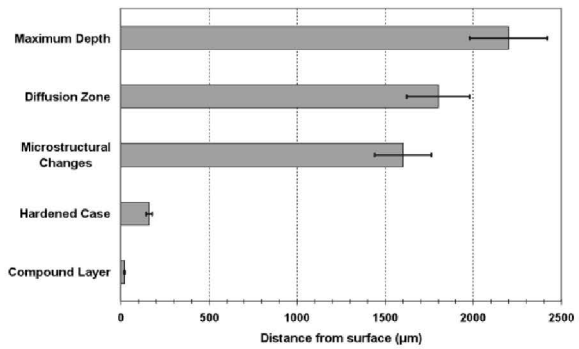

Fig. 10. Main changes of plasma nitrided iron case evaluated by various characterization techniques.

4- Conclusions

Three sections including the compound layer, the diffusion zone, and an intermediate transition zone formed in the plasma nitriding of iron were characterized by microhardness depth profile, optical and scanning electron microscopy, XRD, GDOES, and SIMS techniques. The characterization techniques employed yielded similar results and, thus, provided a reasonable evaluation of nitrogen diffusion in plasma nitrided iron. The main conclusions from this work can be summarized as follows:

- The compound layer consisted of two separated layers including the epsilon and the gamma primes; the thickness of the epsilon nitride was much smaller than that of the gamma prime. The diffusion zone consisted of two mixed regions: one with thick and long needle shaped morphology indexed as the gamma prime nitride, Fe_4N; the second region included thin and uniform precipitates of $Fe_{16}N_2$.
- This surface structure produced a moderate increase in hardness gradient. The hardness of the outer compound layer was above 1000 HV which decreased to less than 300 HV at the transition zone. The hardness gradient decreased smoothly from the transition zone towards the substrate.
- The hardened case depths increased with increasing nitriding time and the case depth measured by optical and electron microscopy was higher than that measured by microhardness depth profile for any given nitriding period.
- The concentration depth profiles characterized by GDOES revealed three sections: at the outer section, nitrogen concentration was very high, indicating that the compound layers were formed. At the inner section, nitrogen concentration decreased to very low values and that of iron increased to nearly 100 percent. The SIMS technique was used for high precision mass concentration depth profiling of nitrogen (below 0.1 wt%) from the surface through the depth of the substrate.
- The results of characterization of plasma nitrided iron, performed by several laboratory methods, indicated good consistency with each other, thus increasing the reliability of the results.
- Nitrogen diffusion depth, detected by SIMS in this work, was higher than 1800 μm, a value not reported in previous works.

5-Acknowledgement

Experimental work performed at Isfahan University of Technology, Maleke-ashtar University of Technology, and The University of Birmingham, assistance by the Iranian Surface Research & Engineering Center for plasma nitriding, and Loughborough Surface Analysis for SIMS analysis are acknowledged. The authors extend their special gratitude to Dr. H. Dong and Dr. X. Li from the Department of Metallurgy and Materials, University of Birmingham, for their cooperation in the GDOES analyses and also to Dr. A. Kermanpur from Isfahan University of Technology for scientific discussions.

References

[1] ASM Committee on Nitriding, Basic coverage of conventional (nitriding) process, in: Source book on nitriding. Metals Park, OH: ASM, 1977, 107.
[2] L. C. Gontijo, R. Machado, E. J. Miola, L. C. Casteletti, P. A. P. Nascente, Surf. Coat. Tech. 183 (2004), 10.
[3] T. Hirsch, T. G. R. Clarke, A. da Silva Rocha, Surf. Coat. Tech., 201 (2007), 6380.
[4] J. Agren, Metall. Mater. Trans. A, 10A (1979), 1847.
[5] K. Frisk, Calphad, 11 (1987), 127.
[6] K. Frisk, Calphad, 15 (1991), 79.
[7] H. Du, J. Phase Equilib., 14 (1993), 682.

[8] H. A. Wriedt, N. A. Gokcen, R. H. Nafziger, Bulletin of Alloys Phase Diagrams, 8 (1997), 355.
[9] S. Malinov, A. J. Bottger, E. J. Mittemeijer, M. I. Pekelharing, M. A. J. Somers, Metall. Mater. Trans. A, 32 (A), 2001, 59.
[10] B. J. Lee, T. H. Lee, S. J. Kim, Acta Mater., 54 (2006), 4597.
[11] G. W. Malaczynski, C. H. Leung, A. A. Elmoursi, A. H. Hamdi, A. B. Campbell, M. P. Balogh, M. C. Militello, S. J. Simko, R. A. Waldo, Mater. Sci. Eng., 289 (1999), 262.
[12] E. J. Mittemeijer, M. A. J. Somers, Surf. Eng., 13 (1997), 483.
[13] H. Du, M. A. J. Somers, J. Agren, Metall. Mater. Trans. A, 31 A (2000), 195.
[14] S. R. Hosseini, F. Ashrafizadeh, Proc. of 7th Seminar on Heat Treatment & Surface Engineering, Isfahan, Iran, (2006), 1591.
[15] S. R. Hosseini, A. Kermanpur, F. Ashrafizadeh, Proc. of the 8th Seminar on Heat Treatment & Surface Engineering, Kerman, Iran, (2007), 571.
[16] S. R. Hosseini, F. Ashrafizadeh, A. Kermanpur, Proc. of the 8th Seminar on Heat Treatment & Surface Engineering, Kerman, Iran, (2007), 563.
[17] Y. Sun, T. Bell, Heat Treat. Met. 24 (1997), 43.
[18] T. Bell, Y. Sun, Proc. of 5th world Seminar on Heat Treatment & Surface Engineering, Isfahan, Iran, (1995), 21
[19] S. R. Hosseini, M. Salehi, Proc. of 5th World Seminar on Heat Treatment & Surface Engineering, Isfahan, Iran, (1995), 81.
[20] M. Salehi and S. R. Hosseini, Surf. Eng., 12 (1996), 221.
[21] P. G. Shewmon Diffusion in Solids.,2nd ed., McGraw-Hill, New York, (1996), 164.